

AD-A053 934

NAVAL POSTGRADUATE SCHOOL MONTEREY CALIF  
COMPARISONS OF ISOGRADIENT-AND ISOSPEED-LAYER MODELS FOR RAY TR--ETC(U)  
APR 78 A B COPPENS

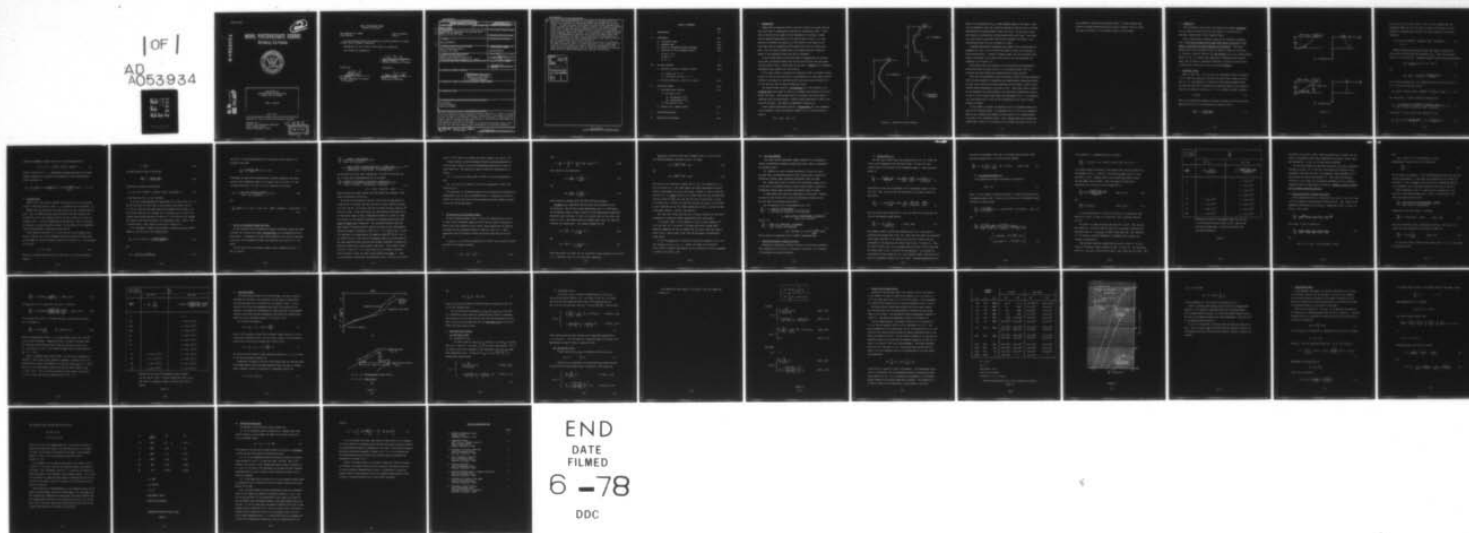
F/G 17/1

UNCLASSIFIED

NPS61-78-004

NL

1 OF 1  
AD  
A053934





2

AD A 053934

# NAVAL POSTGRADUATE SCHOOL

Monterey, California



AD No. \_\_\_\_\_  
DDC FILE COPY

COMPARISONS OF  
ISOGRAIENT-AND ISOSPEED-LAYER  
MODELS FOR RAY TRACING

Alan B. Coppens

April 1978

Approved for public release; distribution unlimited

Prepared for:  
Research and Engineering Department  
Naval Torpedo Station  
Keyport, Washington 98345

DDC  
RECEIVED  
MAY 16 1978  
D

NAVAL POSTGRADUATE SCHOOL  
Monterey, California


Rear Admiral T.F. Dedman  
Superintendent

Jack R. Borsting  
Provost


The work reported herein was supported by funds provided by the Naval Torpedo Station, Keyport, Washington.

Reproduction of all or part of this report is authorized.

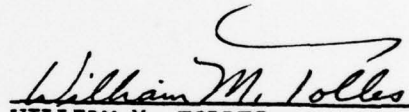
This report was prepared by:

  
ALAN B. COPPENS  
Associate Professor of Physics

Reviewed by:

  
K.E. WOEHLE  
Chairman, Department of Physics  
and Chemistry

Released by:

  
WILLIAM M. TOLLES  
Acting Dean of Research



Unclassified

SECURITY CLASSIFICATION OF THIS PAGE (When Data Entered)

REPORT DOCUMENTATION PAGE		READ INSTRUCTIONS BEFORE COMPLETING FORM
1. REPORT NUMBER 14 NPS61-78-004	2. GOVT ACCESSION NO.	3. RECIPIENT'S CATALOG NUMBER
4. TITLE (and Subtitle) 6 COMPARISONS OF ISOGRADIENT- AND ISOSPEED-LAYER MODELS FOR RAY TRACING,	5. TYPE OF REPORT & PERIOD COVERED	
7. AUTHOR(s) 10 Alan B./Coppens		6. PERFORMING ORG. REPORT NUMBER
9. PERFORMING ORGANIZATION NAME AND ADDRESS Naval Postgraduate School ✓ Monterey, CA 93940		10. PROGRAM ELEMENT, PROJECT, TASK AREA & WORK UNIT NUMBERS N0025378WR00002
11. CONTROLLING OFFICE NAME AND ADDRESS Research Projects Division Research and Engineering Division Naval Torpedo Station, Keyport, WA 98345		12. REPORT DATE 21 APR 78
14. MONITORING AGENCY NAME & ADDRESS (if different from Controlling Office)		13. NUMBER OF PAGES 46 22 44 p.
		15. SECURITY CLASS. (of this report) Unclassified
		15a. DECLASSIFICATION/DOWNGRADING SCHEDULE
16. DISTRIBUTION STATEMENT (of this Report) <div style="border: 1px solid black; padding: 5px; text-align: center;">DISTRIBUTION STATEMENT A Approved for public release; Distribution Unlimited</div>		
17. DISTRIBUTION STATEMENT (of the abstract entered in Block 20, if different from Report)		
18. SUPPLEMENTARY NOTES		
19. KEY WORDS (Continue on reverse side if necessary and identify by block number) Ray Tracing Sound Propagation Acoustical Ranges		
20. ABSTRACT (Continue on reverse side if necessary and identify by block number) If in a stratified ocean an acoustical signal is emitted by a source at a known time and received at another location at a known time, if the angle of arrival of the ray path at the receiver is known, and if the speed of sound profile is known, then the acoustical path from receiver to source can be traced back and the position of the source estimated. The relative accuracies of two models of speed-of-sound profiles used in performing this task are compared. The discrepancies in trace-back between a		

DD FORM 1 JAN 73 1473  
(Page 1)

EDITION OF 1 NOV 65 IS OBSOLETE  
S/N 0102-014-6601

Unclassified  
SECURITY CLASSIFICATION OF THIS PAGE (When Data Entered)

251 454

Unclassified

SECURITY CLASSIFICATION OF THIS PAGE(When Data Entered)

20. speed of sound profile modeled by a succession of isospeed layers and modeled by a succession of isogradient layers are obtained for two situations: (1) when the value of the speed of sound in each isospeed layer is the average over depth of the speed of sound in the analogous isogradient layer, and (2) when the angle of elevation of the ray in the isospeed layer is the average of the entrance and exit angles of the equivalent ray in the analogous isogradient layer. It is found that the second situation leads to discrepancies in range and depth which are always smaller than those encountered in the first, and in particular the discrepancies in the first situation are orders of magnitude smaller than those in the second for cases wherein the rays tend to vertex. The importance of the Snell's law invariant  $(\cos \theta)/c(z)$  is pointed out. Choosing an incorrect value for either the angle  $\theta$  or the actual speed of sound  $c(z)$  at the receiver can lead to errors in localization of the source which are unacceptably large for accurate trace-back in situations where the ray is nearly horizontal over some part of its path.

ACCESSION for	
DTIC	White Section <input checked="" type="checkbox"/>
DDC	Buff Section <input type="checkbox"/>
UNANNOUNCED	<input type="checkbox"/>
JUSTIFICATION.....	
BY.....	
DISTRIBUTION/AVAILABILITY CODES	
Dist.	AVAIL. and/or SPECIAL
A	

Unclassified

SECURITY CLASSIFICATION OF THIS PAGE(When Data Entered)

# TABLE OF CONTENTS

	Page
I. INTRODUCTION	I-1
II. FORMULATION	II-1
A. Isogradient Layer	II-1
B. Isospeed Layer	II-4
C. Ratios of Incremental Ranges and Times	II-6
D. Solutions for the Incremental Angles	II-8
If $\tan^2 \theta \gg D$	
If $\tan^2 \theta \ll h$	
If $\Delta\theta \ll 1$	
III. RAY PATH MATCHING	III-1
A. Matching Criterion in Terms of D and h	III-1
(1) Assume $\tan^2 \theta \gg D$	
(2) All angles, and $\tan^2 \theta \ll 1$	
B. Matching Criterion in Terms of $\Delta\theta$ and $d\theta$	III-6
IV. TRACE-BACK ERRORS	IV-1
A. Trace-Back Error Formulas	IV-3
(1) The Case $h = D/2$	
(a) Calculation of $\Delta t_i$	
(b) Calculation of $\Delta t_i$	
(2) The Case $d\theta = \Delta\theta/2$	
B. Analysis for a Sample Profile	IV-7
V. INITIALIZATION ERROR	V-1
VI. RESULTS AND CONCLUSIONS	VI-1

## I. INTRODUCTION

Assume that an acoustical source initiates a signal at a known time and that this signal is subsequently received by a directional array. If the time of arrival of the signal at each hydrophone of the array is known, and the speed-of-sound profile of the water column is known, it is then possible to determine the angle  $\theta_r$  of the arrival of the signal at the array and trace the trajectory of the signal back over the relevant ray path. With the time of flight known, the original position (range and depth) of the acoustical source can then be estimated.

Of the various sources of error possible in implementing this process, this report is directed toward those arising from the fact that the speed-of-sound profile used in calculating the ray path is modeled on the available experimental data sampling the true profile.

If the water column is divided into horizontal layers, the speed-of-sound profile in each of these layers can be approximated with some simple function of depth which models the observed profile and allows rapid calculation of the ray path and time of flight through that layer.

The simplest model would be a one-parameter fit: the assumption of an isospeed layer whose speed of sound  $c_v$  is obtained from analysis of the data within that layer. The ray path would be a straight line whose angle of elevation would be determined by a layer-by-layer application of Snell's Law along the ray path. This model is suggested in Figure 1.1a.

A more sophisticated model would be a two-parameter fit: the assumption of an isogradient layer whose speed of sound  $c(z)$  is a linear function of depth  $z$ ,

$$c(z) = c(z_0) + g(z - z_0)$$



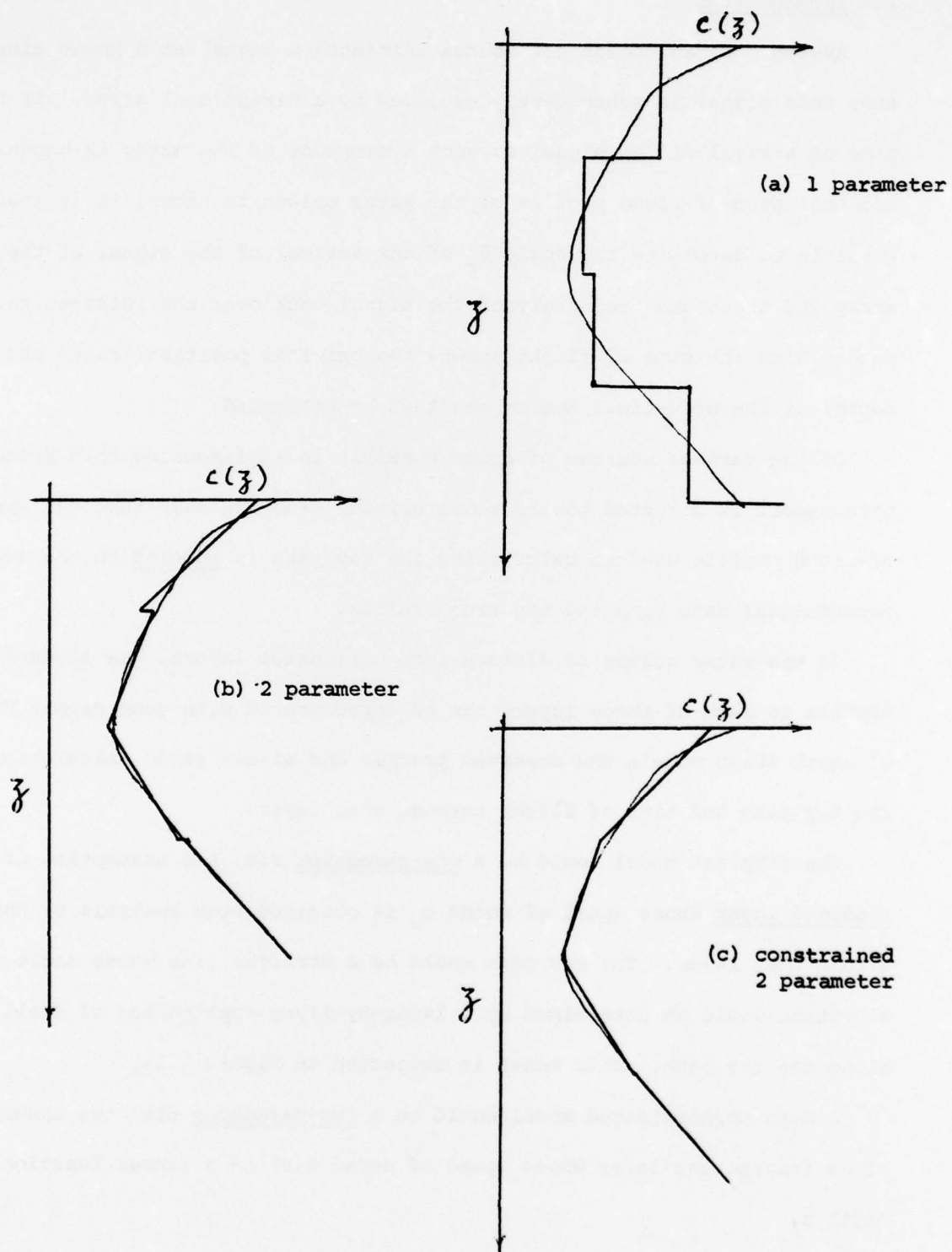


Figure 1.1 Methods of Fitting Profiles

where  $g$  is the gradient and  $z_0$  is some reference depth in the layer. Here, the two parameters  $c(z_0)$  and  $g$  would be obtained by fitting  $c(z)$  to the data representing the observed profile within the layer. The ray path in this case would be a circular arc of fixed radius within each layer. See Figure 1.1b, and notice in particular that the two parameter fit allows  $c$  to be discontinuous across the top or bottom of a layer.

A commonly-encountered isogradient-layer model is the "constrained" two parameter fit (Fig. 1.1c), for which the speed of sound is not allowed to have discontinuities. A moment's thought reveals that this constraint must reduce the accuracy of this model below that of the (unconstrained) two parameter fit of Figure 1.1b.

Other models with more parameters can be postulated (corresponding to fitting the data with power series in  $z$  of increasing order), but the resulting ray paths become more complicated than usually desired.

Given that the experimental data are accurate, models with more parameters would be better capable of reproducing the experimentally determined profile, at least until there are too many parameters for the number of data or until whatever desired smoothing of the data is lost. Below these limits, however, the two-parameter fit should produce a ray path which conforms more closely to that in "real" profile than should the one-parameter fit. It is plausible that this should also be true for the calculations of the time of flight through the layers.

In this report we compare the predictions of the isogradient model with those of two isospeed models. Our approach will be to take the isogradient model as the reference and compare the predictions of two isospeed models with those of the isogradient model. That isospeed model whose predictions conform more closely to the reference will be deemed the better of the two

with respect to locating the acoustical source. We also consider some effects on accurate prediction arising from an incorrect value of either the angle of arrival  $\theta_r$  or the speed of sound  $c_r$  at the array.



## II. FORMULATION

Both isogradient-layer models and isospeed-layer models approximate the true speed-of-sound profile for the purpose of tracing received acoustical signals back to their apparent source.

What is known about a received signal for the situation considered here is the time-of-flight of the signal from source to receiver and the angle  $\theta_r$  with which the signal impinges on the receiver. This angle, together with prior information about the speed of sound at the receiver,  $c_r$ , provides a specific value for the ray invariant  $(\cos \theta_r / c_r)$  which uniquely labels the ray. It follows that comparison of isogradient and isospeed models must be based on studying the different ray paths and travel times resulting from tracing back a ray of specified invariant.

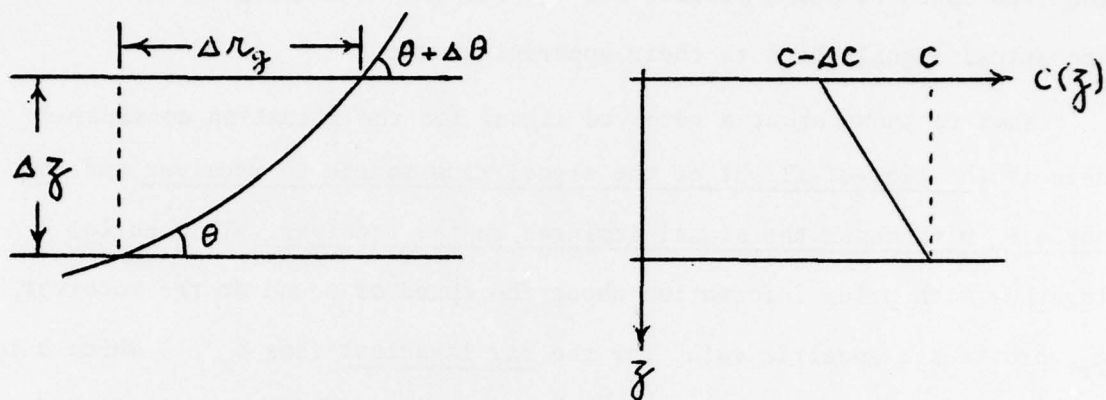
### A. Isogradient Layer

Refer to Fig. 1(a). Let a ray enter an isogradient layer of thickness  $\Delta z$  at an angle of elevation  $\theta$  and leave the layer with an angle of elevation  $\theta + \Delta\theta$ . The gradient  $g$  is defined so that positive-gradient water has speed of sound  $c(z)$  increasing with increasing depth, and the speed of sound at the bottom of the layer is  $c$ . It is useful to define a quantity

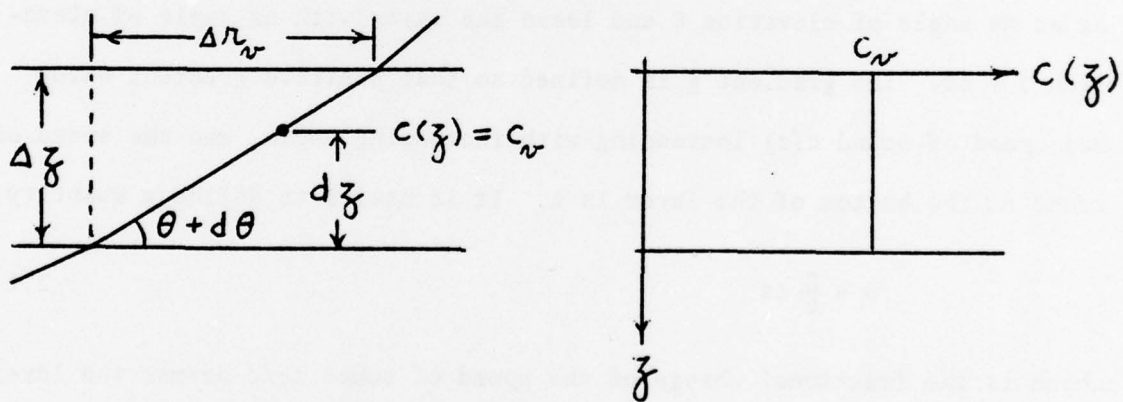
$$D = \frac{g}{c} \Delta z \quad 2.1$$

which is the fractional change of the speed of sound  $\Delta c/c$  across the layer. Application of Snell's Law along the ray relates  $D$  and  $\Delta\theta$ ,

$$\frac{\cos \theta}{c} = \frac{\cos (\theta + \Delta\theta)}{c (1 - D)} \quad 2.2$$



(a) Isogradient Layer



(b) Isospeed Layer

Figure 2.1

Use of  $\cos (\theta + \Delta\theta) = \cos \theta \cos \Delta\theta - \sin \theta \sin \Delta\theta$ , assuming that the incremental angle of  $\Delta\theta$  is very small so that  $\cos \Delta\theta$  and  $\sin \Delta\theta$  can be replaced by truncated power series in  $\Delta\theta$ , and collection of like-order terms gives

$$D = \tan \theta \Delta\theta + (1/2)(\Delta\theta)^2 - (1/6) \tan \theta (\Delta\theta)^3 - (1/24) (\Delta\theta)^4 + \dots \quad 2.3$$

$$\Delta\theta \ll 1.$$

Between entering and leaving the layer the range has increased by  $\Delta r_g$ , and the time-of-flight has increased by  $\Delta t_g$ . Since the ray path is a section of a circular arc, elementary analysis yields the known expressions

$$\Delta r_g = \frac{c}{g \cos \theta} [\sin (\theta + \Delta\theta) - \sin \theta] \quad 2.4$$

and

$$\Delta t_g = \frac{1}{g} \ln \left[ \frac{c}{c(1 - D)} \frac{1 + \sin (\theta + \Delta\theta)}{1 + \sin \theta} \right] . \quad 2.5$$

In the first expression, Eq. 2.4, expansion of the first sine and use of  $\Delta\theta \ll 1$  results in the power series

$$\Delta r_g = \frac{c}{g} [\Delta\theta - (1/2) \tan \theta (\Delta\theta)^2 - (1/6) (\Delta\theta)^3 + (1/24) \tan \theta (\Delta\theta)^4 + \dots] . \quad 2.6$$

Now, use of Eqs. 2.1 and 2.3 yields the desired form

$$\Delta r_g = \frac{1 - (1/2) \tan \theta \Delta\theta - (1/6) (\Delta\theta)^2 + (1/24) \tan \theta (\Delta\theta)^3 + \dots}{\tan \theta + (1/2) \Delta\theta - (1/6) \tan \theta (\Delta\theta)^2 - (1/24) (\Delta\theta)^3 + \dots} \Delta z. \quad 2.7$$

To cast Eq. 2.5 into a useful form, separate it into

$$\Delta t_g = \frac{1}{g} \left\{ \ln \left[ \frac{1 + \sin (\theta + \Delta\theta)}{1 + \sin \theta} \right] - \ln \left[ \frac{\cos (\theta + \Delta\theta)}{\cos \theta} \right] \right\} , \quad 2.8$$

expand the arguments in power series in  $\Delta\theta$ , and then make use of

$$\ln(1+x) = x - (1/2)x^2 + (1/3)x^3 - (1/4)x^4 + \dots \quad 2.9$$

which is valid for  $|x| < 1$ . Combination of these steps and use of trigonometric identities to simplify the coefficients in the resulting power series culminates in

$$\Delta t_g = \frac{1}{g} \left[ \frac{1}{\cos \theta} \Delta\theta + (1/2) \frac{\tan \theta}{\cos \theta} (\Delta\theta)^2 + (1/6) \frac{1 + \sin^2 \theta}{\cos^3 \theta} (\Delta\theta)^3 + \dots \right]. \quad 2.10$$

#### B. Isospeed Layer

Refer to Fig. 1(b) and now consider the properties of a ray traversing a layer in which the speed of sound  $c_v$  is constant over its thickness  $\Delta z$ .

(Recall that for both models the same value of the ray invariant must be used. Thus, we assume that  $(\cos \theta_r)/c_r$  has exactly the same value for the straight-line ray in the isospeed layer as for the circular arc in the isogradient layer. As we have formulated the problem here, this is equivalent to relating  $c_v$  to both the speed of sound  $c$  at the bottom of the isogradient layer and the gradient  $g$  found within that layer.)

If the angle of elevation is  $\theta + d\theta$  for the ray in the isospeed layer, then the circular arc in the isogradient layer will possess the same slope at that depth for which the speed of sound  $c(z)$  is equal to  $c_v$ . This provides the relation

$$c_v = c \left( 1 - \frac{g}{c} dz \right) \quad 2.11$$

where  $dz$  is measured from the bottom of the layer. Use of the convenient quantity

$$h = \frac{g}{c} dz \quad 2.12$$

and application of Snell's Law yields

$$\frac{\cos \theta}{c} = \frac{\cos (\theta + d\theta)}{c (1 - h)} \quad 2.13$$

from which we extract the expression

$$h = \tan \theta d\theta + (1/2)(d\theta)^2 - (1/6)\tan \theta (d\theta)^3 - (1/24)(d\theta)^4 + \dots \quad 2.14$$

in the same way as Eq. 2.3 was obtained.

As an aid in understanding the significance of  $h$ , notice that if  $h = 0$ , the two rays have the same slope at the bottoms of the layers, and if  $h = D/2$ , the rays have the same slope at the middles of the layers. For this latter condition, the straight ray is traveling as if it were in an isospeed layer possessing speed of sound  $c(1 - D/2)$ , which is the average over depth of the speed of sound in the isogradient layer. Notice that, as defined above,  $h$  must always be less than or equal to  $D$ .

It is elementary to obtain the increment in range  $\Delta r_v$  and the time-of-flight  $\Delta t_v$  for the ray in the isospeed layer:

$$\Delta r_v = \cot (\theta + d\theta) \Delta z = \frac{1 - \tan \theta \tan d\theta}{\tan \theta + \tan d\theta} \Delta z \quad 2.15$$

and

$$\Delta t_v = \frac{1}{c (1 - h)} \frac{\Delta z}{\sin (\theta + d\theta)} \quad 2.16$$



Use of Eq. 2.13 and the definition of D allows the time-of-flight to be written in the form

$$\frac{1}{\Delta t_v} = \frac{g}{D} \frac{\cos (\theta + d\theta)}{\cos \theta} \sin (\theta + d\theta) \quad . \quad 2.17$$

Performing the same kind of manipulations as before (expansion into power series in the incremental angle, use of Snell's Law, use of Eq. 2.3, and so forth) allows Eqs. 2.15 and 2.17 to be rewritten in the forms

$$\Delta t_v = \frac{1 - \tan \theta d\theta - (1/3)\tan \theta (d\theta)^3 + \dots}{\tan \theta + d\theta + (1/3)(d\theta)^3 + \dots} \Delta z \quad 2.18$$

and

$$\frac{1}{\Delta t_v} = \frac{g}{D} \sin \theta [1 + (\cot \theta - \tan \theta) d\theta - 2(d\theta)^2 - (2/3)(\cot \theta - \tan \theta)(d\theta)^3 + \dots]. \quad 2.19$$

### C. Ratios of Incremental Ranges and Times

We are concerned with the differences between incremental ranges and times-of-flight for ray paths with equal ray invariants in the isogradient and iso-speed layers. Investigation of these small differences will reveal techniques to minimize the discrepancies between the range and time results of the two models.

For the ratio of the incremental ranges, direct combination of Eqs. 2.7 and 2.18 yields

$$\frac{\Delta r_v}{\Delta r_g} = \frac{1 - \tan\theta d\theta - (1/3)\tan\theta(d\theta)^3 + \dots}{\tan\theta + d\theta + (1/3)(d\theta)^3 + \dots} \times \frac{\tan\theta + (1/2)\Delta\theta - (2/3)\tan\theta[(1/2)\Delta\theta]^2 - (1/3)[(1/2)\Delta\theta]^3 + \dots}{1 - \tan\theta[(1/2)\Delta\theta] - (2/3)[(1/2)\Delta\theta]^2 + (1/3)\tan\theta[(1/2)\Delta\theta]^3 + \dots} \quad 2.20$$

For the ratio of travel times, combine Eqs. 2.10 and 2.19 and then use Eq. 2.3 (the series representation for D) to obtain

$$\frac{\Delta t_g}{\Delta t_v} = \frac{\tan\theta\Delta\theta[1 + (1/2)\tan\theta\Delta\theta + (1/6)(\sec^2\theta + \tan^2\theta)(\Delta\theta)^2 + \dots]}{\tan\theta\Delta\theta + (1/2)(\Delta\theta)^2 - (1/6)\tan\theta(\Delta\theta)^3 - (1/24)(\Delta\theta)^4 + \dots} \quad 2.21$$

$$\times [1 + (\cot\theta - \tan\theta)d\theta - 2(d\theta)^2 + \dots].$$

Study of these two ratios reveals that they depend very strongly on the angle of elevation  $\theta$  of the ray.

As an aid in the analysis to follow, notice that for all angles of elevation Eq. 2.3 reveals that the term  $\tan\theta \cdot \Delta\theta$  must always be of order D or less, and Eq. 2.14 reveals that  $\tan\theta \cdot d\theta$  must similarly always be of order h or less. On the other hand, the terms  $\Delta\theta/(\tan\theta)$  and  $d\theta/(\tan\theta)$  can be arbitrarily large or small, depending on whether  $\theta$  is small or large. As a result, it will often be necessary to investigate these ratios for large and small angles separately. The distinction between large and small angles of elevation must be made on the basis of the relationships between the angle of elevation  $\theta$  and D or h. It is seen for Eqs. 2.3 and 2.14 that when  $\theta$  is reduced until it becomes of order  $D^{1/2}$  (in Eq. 2.3) or of order  $h^{1/2}$  (in Eq. 2.14) then the incremental angles  $\Delta\theta$  and  $d\theta$  become of the same respective orders and the terms  $d\theta/(\tan\theta)$  and  $\Delta\theta/(\tan\theta)$  change from being less than unity to being greater than unity. Since typical values of D are of order  $10^{-4}$ , it is clear that the two extremes of behavior occur for angles  $\theta$  much less than or much greater than about  $1^\circ$ . Thus, it is necessary to investigate the behaviors of Eqs. 2.20 and 2.21 for the



cases  $\theta \ll h^{\frac{1}{2}}$  (since  $h$  is always less than or equal to  $D$ ), and  $\theta \gg D^{\frac{1}{2}}$ .

In what follows, we must distinguish between measuring quantities in terms of their orders in  $\Delta\theta$  and  $d\theta$  and measuring quantities in terms of their order in  $D$ . The notation we adopt to make this distinction is as follows:

(1) If a term is of order  $(\Delta\theta)^n$  or  $(d\theta)^n$ , it will be represented by  $O(n)$ .

(2) If a term is of order  $D^n$ , it will be represented by  $O(D^n)$ , and similarly for  $h$ .

The expansions in incremental angles will be convenient for mathematical manipulations, but it must be remembered that it is expansion in orders of  $D$  which will reveal the sizes of the discrepancies between ranges and times for the two ray-tracing models.

#### D. Solutions for the Incremental Angles

We have already obtained in Eqs. 2.3 and 2.14 expressions for  $D$  and  $h$  in terms of the incremental angles  $\Delta\theta$  and  $d\theta$  and the angle of elevation  $\theta$ . Since  $D$  and  $h$  are constants for the layers, these expressions are implicit solutions for the incremental angles in terms of  $\theta$  and  $D$  or  $h$ . These expressions must be inverted to obtain the desired equations for  $\Delta\theta$  and  $d\theta$ .

If  $\tan^2 \theta \gg D$ , the series expansions for  $D$  and  $h$  can be reverted directly by means of the standard formula:

If

$$y = a_1x + a_2x^2 + a_3x^3 + \dots \quad 2.22$$

then

$$x = \frac{1}{a_1} y - \frac{a_2}{a_1^3} y^2 + \frac{1}{a_1^5} (2 a_2^2 - a_1 a_3) y^3 + \dots \quad 2.23$$

This results in the expressions

$$\Delta\theta = \frac{D}{\tan \theta} - \frac{1}{2} \frac{D^2}{\tan^3 \theta} + \dots \quad 2.24$$

and

$$d\theta = \frac{h}{\tan \theta} - \frac{1}{2} \frac{h^2}{\tan^3 \theta} + \dots \quad 2.25$$

where terms just through  $O(D^2)$  and  $O(h^2)$  have been retained.

If  $\tan^2 \theta \ll h$ , expressions for  $\Delta\theta$  and  $d\theta$  can be obtained in the following way: Use the small angle approximation  $\tan \theta \doteq \theta$  and express the incremental angles as power series in  $\theta$  with undetermined coefficients. Substitute these into Eqs. 2.3 and 2.14, collect terms of like order, and equate to zero. This reveals that the assumed power series are valid and evaluates the coefficients. The results through  $O(2)$  are

$$\Delta\theta = \sqrt{2D} - \theta + \frac{1}{2\sqrt{2D}} \theta^2 - \dots \quad 2.26$$

and

$$d\theta = \sqrt{2h} - \theta + \frac{1}{2\sqrt{2h}} \theta^2 - \dots \quad 2.27$$

These expressions are useful for the validation of some equations in the limit  $\theta \rightarrow 0$ . Otherwise, they are of no practical importance.

If  $\Delta\theta \ll 1$ , then  $O(3)$  terms can be dropped in Eqs. 2.3 and 2.14 and the resulting quadratic equations solved. We obtain

$$\Delta\theta \doteq \sqrt{\tan^2 \theta + 2D} - \tan \theta \quad 2.28$$

and

$$d\theta \doteq \sqrt{\tan^2 \theta + 2h} - \tan \theta . \quad 2.29$$

Note that for the situations studied here ( $D \ll 1$ ), the condition  $\Delta\theta \ll 1$  will be met for all  $\theta$ . (It might appear that these approximate solutions would be questionable when  $\tan \theta$  gets large. However, it must be recalled that  $\tan \theta \cdot \Delta\theta$  is always of  $O(D)$  or less which means that the discarded  $O(3)$  term will always be  $O(D)$  less than the  $O(2)$  term in each of Eqs. 2.3 and 2.14.) While Eqs. 2.28 and 2.29 could be used for all angles, it will often be more convenient to use the simpler forms given by Eqs. 2.24 and 2.25 for large angles and Eqs. 2.28 and 2.29 otherwise.

This last case, being valid for all  $\theta$ , allows evaluation of the errors encountered in using the simpler approximations for large angles.

If we assume  $\tan^2 \theta \gg D$  and expand Eq. 2.28 in a power series in  $D$ , it is seen that Eq. 2.28 and Eq. 2.24 agree identically through  $O(D^2)$ . Numerical comparison of the two formulas for  $\Delta\theta$  reveals that they agree to within 0.5% as long as  $\tan^2 \theta \geq 10D$ , with the discrepancy decreasing for larger angles.

If just the first term is retained in the series expansion of Eq. 2.24 then agreement with Eq. 2.28 is within 0.5% under the restriction  $\tan^2 \theta \geq 100D$ ; of greater significance for the discussion to follow, agreement is within 5% for  $\tan^2 \theta \geq 10D$ .

### III. RAY PATH MATCHING

Two rather obvious approaches suggest themselves in attempting to reduce the differences between ray paths and travel times in isogradient and isospeed layers:

(A) Express the ratios obtained previously in terms of D and h and then find a relationship between D and h which tends to reduce the differences between range increments and between times of flight.

(B) Expand these ratios in terms of the incremental angles  $\Delta\theta$  and  $d\theta$  and find a relationship between  $\Delta\theta$  and  $d\theta$  which tends to reduce the differences between range increments and between times of flight.

It might appear that these two approaches are equivalent. However, we shall see that there will be distinct differences between the two when the angle of elevation becomes small.

The two equations to be investigated are Eq. 2.20

$$\frac{\Delta t_v}{\Delta t_g} \doteq \frac{1 - \tan\theta d\theta - (1/3)\tan\theta(d\theta)^3}{1 - (1/2)\tan\theta \Delta\theta - (1/6)(\Delta\theta)^2 + (1/24)\tan\theta(\Delta\theta)^3} \quad 3.1$$

$$\times \frac{\tan\theta + (1/2)\Delta\theta - (1/6)\tan\theta(\Delta\theta)^2 - (1/24)(\Delta\theta)^3}{\tan\theta + d\theta + (1/3)(d\theta)^3}$$

and Eq. 2.21

$$\frac{\Delta t_g}{\Delta t_v} \doteq \frac{\tan\theta + (1 - \tan^2\theta) d\theta - 2 \tan\theta(d\theta)^2}{\tan\theta + (1/2)\Delta\theta - (1/6)\tan\theta(\Delta\theta)^2} \quad 3.2$$

$$\times [1 + (1/2)\tan\theta \Delta\theta + (1/6) \frac{1 + \sin^2\theta}{\cos^2\theta} (\Delta\theta)^2]$$

both of which are expressed here in slightly rearranged forms.

#### A. Matching Criterion in Terms of D and h

Because the expressions relating  $\Delta\theta$  and  $d\theta$  to D and h have different forms depending on the values of the angle of elevation, it is necessary to investigate each regime separately.



(1) Assume  $\tan^2\theta \gg D$

For this case, retain terms just through  $O(2)$  in Eq. 3.1, revert the series in the denominator with the help of Eqs. 2.22 and 2.23, and collect terms of like powers of the incremental angles. These operations result in

$$\frac{\Delta r_v}{\Delta r_g} \doteq 1 + \frac{(1/2)\Delta\theta - d\theta}{\sin\theta\cos\theta} + [(1/4)\frac{(\Delta\theta)^2}{\cos^2\theta} + \frac{(d\theta)^2}{\sin^2\theta} - (1/2)\frac{\Delta\theta d\theta}{\sin^2\theta\cos^2\theta}]. \quad 3.3$$

Substitution of the series expansions of the incremental angles in terms of  $D$  and  $h$  (Eqs. 2.24 and 2.25) and collection of like-order terms in  $D$  and  $h$  gives

$$\frac{\Delta r_v}{\Delta r_g} \doteq 1 + (1/2)\frac{D - 2h}{\sin^2\theta} + (1/4)\left[\frac{D^2}{\sin^2\theta} + \frac{6h^2 - D^2}{\sin^2\theta\tan^2\theta} - \frac{2Dh}{\sin^4\theta}\right]. \quad 3.4$$

The first order term vanishes for  $h = D/2$ , and under this restriction the ratio of incremental ranges becomes

$$\frac{\Delta r_v}{\Delta r_g} \doteq 1 - \frac{1}{8}\frac{D^2}{\tan^2\theta\sin^2\theta}, \quad \tan^2\theta \geq 10D. \quad 3.5$$

The condition  $\tan^2\theta \geq 10D$  for the validity of Eq. 3.5 is the result of retaining just through  $O(2)$  in Eq. 3.3: When  $(\Delta\theta)^2$  and  $(d\theta)^2$  are calculated, terms higher than  $O(2)$  in the results must also be discarded, but this corresponds to retaining just the first terms in Eqs. 2.24 and 2.25. Thus, the term of  $O(D^2)$  in Eq. 3.5 is accurate only for values of  $\tan\theta$  such that the second terms in Eqs. 2.24 and 2.25 are negligible. As discussed in the previous section (after Eq. 2.9), this requires  $\tan^2\theta \geq 10D$  for the  $O(2)$  term to be accurate to about 10% of its value. Analogous manipulations for

the ratio of incremental times (Eq. 3.2) reveals that the first order term also vanishes for  $h = D/2$  and the ratio becomes

$$\frac{\Delta t_g}{\Delta t_v} \doteq 1 + \frac{1}{8} \frac{D^2}{\sin^2 \theta} \left( \frac{1}{\tan^2 \theta} + \frac{2}{3} - 2 \cos^2 \theta \right), \quad \tan^2 \theta \geq 10D. \quad 3.6$$

(2) All angles, and  $\tan^2 \theta \ll 1$

If we represent the angle of elevation in terms of  $D$ ,

$$\tan^2 \theta = yD \quad 3.7$$

where  $y$  is the variable, substitute into Eqs. 3.1 and 3.2, and express the incremental angles by Eqs. 2.28 and 2.29, the ratios of incremental ranges and times of flight become

$$\frac{\Delta r_v}{\Delta r_g} = \frac{1}{2} \frac{\sqrt{1 + 2/y} + 1}{\sqrt{1 + 1/y}} [1 - yD(\sqrt{1 + 1/y} - \sqrt{1 + 2/y}/2 - 1/2)] \quad 3.8$$

and

$$\begin{aligned} \frac{\Delta t_g}{\Delta t_v} &= \frac{\sqrt{1 + 1/y} - yD(3 - 3\sqrt{1 + 1/y} + 2/y)}{(1/2)(\sqrt{1 + 2/y} + 1) - (1/3)yD(1 - \sqrt{1 + 2/y} + 1/y)} \\ &\times \left[ 1 + (1/6)yD(1 - \sqrt{1 + 2/y} + 2/y) \right. \\ &\quad \left. + (2/3)(yD)^2 (1 - \sqrt{1 + 2/y} + 1/y) \right]. \quad 3.9 \end{aligned}$$

If we assume  $y \gg 1$ , expansion of Eq. 3.8 yields

$$\frac{\Delta r_v}{\Delta r_g} = 1 - \frac{1}{8} (1/y^2 + D/y - D^2/3) + O(1/y^3, D/y^2, D^2/y, D^3) + \dots$$

If we desire about 10% accuracy in the second term, then  $D/y$  and  $D^2/3$  can be discarded if  $D/y < 1/(10 y^2)$ . This gives an upper limit to  $\theta$  such that  $\tan^2 \theta \leq 1/10$ . Analysis of Eq. 3.9 is similar and leads to about the same upper limit on  $\tan^2 \theta$ . Thus, for angles satisfying this inequality, Eqs. 3.8 and 3.9 can be simplified to

$$\frac{\Delta r_v}{\Delta r_g} = (1/2) \frac{\sqrt{\tan^2 \theta + 2D} + \tan \theta}{\sqrt{\tan^2 \theta + D}} \quad \tan^2 \theta \leq 1/10 \quad 3.10$$

and

$$\frac{\Delta t_g}{\Delta t_v} = (\Delta r_v / \Delta r_g)^{-1} \quad \tan^2 \theta \leq 1/10. \quad 3.11$$

For the upper bound on  $\theta$  in Eqs. 3.10 and 3.11 to overlap the lower bound on  $\theta$  in Eqs. 3.5 and 3.6, we must have  $1/10 \geq 10D$  which requires  $D \leq 10^{-2}$ .

(If there is a range of angles such that  $1/10 < \tan^2 \theta < 10D$ , then the full forms Eqs. 3.8 and 3.9 must be used if it is desired to estimate the fractional error  $[1 - (\Delta r_v / \Delta r_g)]$  to better than about 10%. The condition  $D \sim 10^{-2}$  would be virtually impossible to encounter when accurate ray tracing is being done.)

Some pertinent numerical comparisons are given in Table 3.1 for the ratios of incremental ranges predicted by Eqs. 3.5 and 3.10. The fractional errors are consistent within 20% for  $\tan^2 \theta \geq 10D$ , within 10% for  $\tan^2 \theta \geq 20D$ ,



$h = D/2$	$\frac{\Delta t_v}{\Delta t_g}$	
	Eq. 3.5	Eq. 3.10
$\frac{\tan^2 \theta}{D}$	$1 - \frac{1}{8} \frac{D^2}{\tan^2 \theta \sin^2 \theta}$	$\frac{1}{2} \frac{\sqrt{\tan^2 \theta + 2D} + \tan \theta}{\sqrt{\tan^2 \theta + D}}$
0	-	$1 - 2.93 \times 10^{-1}$
1	-	$1 - 3.41 \times 10^{-2}$
2	-	$1 - 1.44 \times 10^{-2}$
5	-	$1 - 3.50 \times 10^{-3}$
10	$1 - 1.25 \times 10^{-3}$	$1 - 1.04 \times 10^{-3}$
20	$1 - 3.13 \times 10^{-4}$	$1 - 2.84 \times 10^{-4}$
50	$1 - 5.00 \times 10^{-5}$	$1 - 4.81 \times 10^{-5}$
100	$1 - 1.25 \times 10^{-5}$	$1 - 1.23 \times 10^{-5}$

Comparison of ratios of incremental ranges for the case  $h = D/2$  and the restriction  $\tan^2 \theta \leq 1/10$ . [The ratios of times-of-flight (Eqs. 3.5 and 3.10) deviate from each other similarly.]

Table 3.1

and within 1% for  $\tan^2\theta \geq 100D$ . Similar calculations, not shown, for the ratios of incremental times reveal comparable, but slightly better, agreement between Eqs. 3.6 and 3.11 at each value of  $(\tan^2\theta)/D$ .

For very small angles the fractional deviations are quite significant: From Eqs. 3.10 and 3.11, if the ray is horizontal at the bottom of the isogradient layer then the ratio of incremental ranges approaches  $1/\sqrt{2}$  and the ratio of travel times becomes  $\sqrt{2}$ . Thus, while the matching criterion  $h = D/2$  yields very satisfactory agreement for the incremental ranges and times at large angles of elevation, agreement becomes extremely poor for angles approaching grazing.

#### B. Matching Criterion in Terms of $\Delta\theta$ and $d\theta$

Direct examination of Eq. 3.1 shows that if we set  $d\theta = \Delta\theta/2$ , all terms of  $O(1)$  in numerator and denominator become identical. Now, return to the fundamental definitions of  $\Delta\tau_v$  and  $\Delta\tau_g$ : Combination of Eqs. 2.4 and 2.15 with  $d\theta = \Delta\theta/2$  yields

$$\frac{\Delta\tau_v}{\Delta\tau_g} = \frac{\cos\theta}{\tan(\theta + \Delta\theta/2)} \frac{1}{\sin(\theta + \Delta\theta) - \sin\theta} \frac{g\Delta z}{c} .$$

Use of Eqs. 2.1 and 2.2 results in

$$\frac{\Delta\tau_v}{\Delta\tau_g} = \frac{\cos(\theta + \Delta\theta/2)}{\sin(\theta + \Delta\theta/2)} \frac{\cos\theta - \cos(\theta + \Delta\theta)}{\sin(\theta + \Delta\theta) - \sin\theta} . \quad 3.12$$

Now,

$$\sin(\theta + \Delta\theta) - \sin\theta = 2 \sin(\Delta\theta/2)\cos(\theta + \Delta\theta/2)$$

and

$$\cos\theta - \cos(\theta + \Delta\theta) = 2 \sin(\Delta\theta/2) \sin(\theta + \Delta\theta/2).$$

Substitution of these into Eq. 3.12 shows that

$$\frac{\Delta t_v}{\Delta t_g} = 1 \quad 3.13$$

for all angles of elevation. (It is worth pointing out that this can also be seen from geometry: In the layer the straight-line ray of angle of elevation  $\theta + \Delta\theta/2$  is tangent to the circular arc, subtending angle  $\Delta\theta$ , at its midpoint, and is therefore parallel to the chord of the arc.)

Direct examination of Eq. 3.2 shows that the criterion  $d\theta = \Delta\theta/2$  similarly causes terms through  $O(1)$  to vanish. Substitution of this choice and simplification yields

$$\frac{\Delta t_g}{\Delta t_v} = \frac{\tan\theta + (1/2)\Delta\theta + (1/12)\tan\theta(\tan^2\theta - 1)(\Delta\theta)^2}{\tan\theta + (1/2)\Delta\theta - (1/6)\tan\theta(\Delta\theta)^2} \quad 3.14$$

Examination of the limit  $\tan^2\theta \gg D$  reveals

$$\frac{\Delta t_g}{\Delta t_v} = 1 + (1/12)(\tan^2\theta + 1)(\Delta\theta)^2, \quad \tan^2\theta \geq 10D \quad 3.15$$

where the restriction  $\tan^2\theta \geq 10D$  follows as before. Use of Eq. 2.24 allows the above expression to be stated in terms of  $D$ ,

$$\frac{\Delta t_g}{\Delta t_v} = 1 + (1/12) \frac{D^2}{\sin^2\theta}, \quad \tan^2\theta \geq 10D \quad 3.16$$

At the other extreme, under the restriction  $\tan^2\theta \ll 1$ , Eq. 3.14 assumes the approximate form

$$\frac{\Delta t_g}{\Delta t_v} = 1 + (1/6) \tan \theta \frac{(\Delta \theta)^2}{2 \tan \theta + \Delta \theta}, \quad \tan^2 \theta \leq 1/10. \quad 3.17$$

To express Eq. 3.17 in terms of D, use of Eq. 2.28 gives

$$\frac{\Delta t_g}{\Delta t_v} = 1 + (1/6) \tan \theta \frac{(\sqrt{\tan^2 \theta + 2D} - \tan \theta)^2}{\sqrt{\tan^2 \theta + 2D} + \tan \theta}, \quad \tan^2 \theta \leq 1/10. \quad 3.18$$

In the range  $10D < \tan^2 \theta < 1/10$  where both Eqs. 3.16 and 3.18 are valid, Eq. 3.18 reduces to

$$\frac{\Delta t_g}{\Delta t_v} = 1 + (1/12) \frac{D^2}{\tan^2 \theta}, \quad 10D < \tan^2 \theta < 1/10. \quad 3.19$$

Within the approximation  $\tan^2 \theta \ll 1$ , for which  $\tan \theta \doteq \sin \theta$ , Eqs. 3.18 and 3.16 are thus equivalent. Comparison of Eqs. 3.16 and 3.19 reveals that the fractional error between travel times are consistent within 10% if  $[1 - (\tan \theta / \sin \theta)^2] \leq 1/10$ . This yields the upper limit on  $\tan^2 \theta$  stated in Eqs. 3.17 - 3.19.

Table 3.2 presents some values of Eqs. 3.16 and 3.18 as functions of  $(\tan^2 \theta)/D$ . Notice that  $\Delta t_g / \Delta t_v$  exhibits a maximum. Analysis of Eq. 3.18 reveals that it occurs for  $(\tan^2 \theta)/D = 1/4$  and has value  $\Delta t_g / \Delta t_v = 1 + D/24$ . For  $D = 2 \times 10^{-4}$  the maximum value of the ratio of travel times is thus  $1 + 8.33 \times 10^{-6}$ . This is in clear contrast with the results of the case  $h = D/2$  for which the ratio has maximum value  $\sqrt{2}$  at  $\theta = 0$ .

$d\theta = \Delta\theta/2$	$\frac{\Delta t_g}{\Delta t_v}$	
	Eq. 3.16	Eq. 3.18
$\frac{\tan^2\theta}{D}$	$1 + \frac{1}{12} \frac{D^2}{\sin^2\theta}$	$1 + \frac{1}{6} \tan\theta \frac{(\sqrt{\tan^2\theta + 2D} - \tan\theta)^2}{\sqrt{\tan^2\theta + 2D} + \tan\theta}$
0	-	1 + 0
0.01	-	1 + 1.91 x 10 <sup>-2</sup> D
0.02	-	1 + 2.47 x 10 <sup>-2</sup> D
0.05	-	1 + 3.29 x 10 <sup>-2</sup> D
0.1	-	1 + 3.83 x 10 <sup>-2</sup> D
0.2	-	1 + 4.14 x 10 <sup>-2</sup> D
0.5	-	1 + 3.93 x 10 <sup>-2</sup> D
1	-	1 + 3.27 x 10 <sup>-2</sup> D
10	1 + 8.33 x 10 <sup>-3</sup> D	1 + 7.25 x 10 <sup>-3</sup> D
20	1 + 4.17 x 10 <sup>-3</sup> D	1 + 3.88 x 10 <sup>-3</sup> D
50	1 + 1.67 x 10 <sup>-3</sup> D	1 + 1.62 x 10 <sup>-3</sup> D
100	1 + 8.33 x 10 <sup>-4</sup> D	1 + 8.21 x 10 <sup>-4</sup> D

Comparisons of ratios of incremental times-of-flight

for the case  $d\theta = \Delta\theta/2$  and the restriction  $\tan^2\theta \leq 1/10$ .

The ratio of incremental ranges is exactly unity for all angles.

Table 3.2



#### IV. TRACE-BACK ERRORS

Given the time-of-flight of the received signal, the value of the ray invariant over the path it has travelled, and the speed of sound profile, the received signal can be traced back to its apparent source. In this section we will treat the isogradient-layer model of the profile as our reference, and compare the discrepancies in range and depth of the apparent location of the source between isogradient-layer models and isospeed-layer models for the two matching criteria  $h = D/2$  and  $d\theta = \Delta\theta/2$ .

Let us define the quantity

$$\Delta r_i = \Delta r_{gi} - \Delta r_{vi} = \Delta r_{gi} \left( 1 - \frac{\Delta r_{vi}}{\Delta r_{gi}} \right) \quad 4.1$$

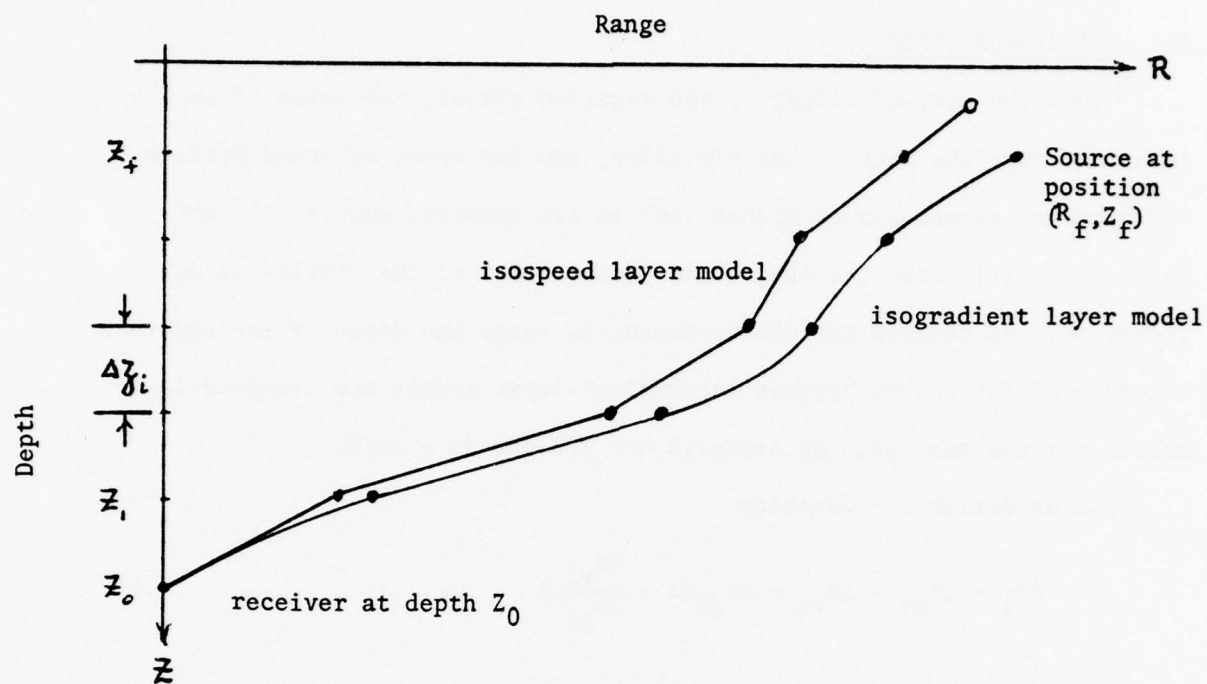
which is the discrepancy between the incremental ranges obtained in the  $i$ th isospeed and isogradient layers, and the similar quantity for the difference between the times-of-flight through each of these layers,

$$\Delta t_i = \Delta t_{gi} - \Delta t_{vi} = \Delta t_{vi} \left( \frac{\Delta t_{gi}}{\Delta t_{vi}} - 1 \right) . \quad 4.2$$

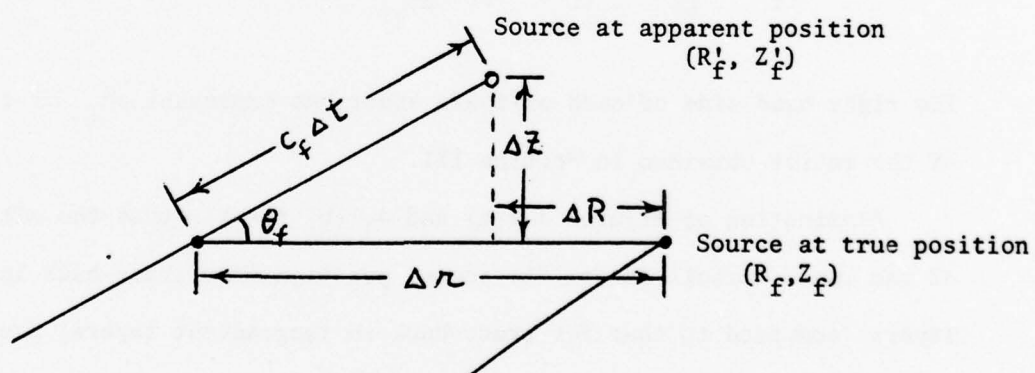
The right hand side of each of these equations expresses  $\Delta r_i$  or  $\Delta t_i$  in terms of the ratios obtained in Section III.

Examination of Figures 4.1(a) and 4.1(b) reveals that the altitude excess  $\Delta Z$  and range deficit  $\Delta R$  for the source position from trace-back in isospeed layers (compared to that for trace-back in isogradient layers) are

$$\Delta Z = c_f \sin \theta_f \sum_{i=1}^f \Delta t_i \quad 4.3$$



(a)



$$\Delta Z = z_f - z'_f = \text{altitude excess (depth deficit)}$$

$$\Delta R = R_f - R'_f = \text{range deficit}$$

(b)

Figure 4.1



and

$$\Delta R = \sum_{i=1}^f \Delta r_i - \cot \theta_f \Delta Z \quad 4.4$$

where  $c_f$  and  $\theta_f$  are the speed of sound and angle of elevation of the ray in the last isospeed layer.

Since we have usually expressed  $\Delta r_{vi}/\Delta r_{gi}$  and  $\Delta t_{gi}/\Delta t_{vi}$  in the form  $[1 + (\text{correction term})_i]$  where the correction term is found to reasonably high accuracy, we can in what follows relax the rigor maintained up to this point, since we are concerned more with the approximate sizes of  $\Delta R$  and  $\Delta Z$  rather than their precise values.

#### A. Trace-Back Error Formulas

##### (1) The Case $h = D/2$ .

##### (a) Calculation of $\Delta r_i$ :

For  $\tan^2 \theta \geq 10D$ , we find  $\Delta r_{vi}/\Delta r_{gi}$  from Eq. 3.5, and  $\Delta r_{gi} \doteq \Delta z_i \cot \theta_i$  from Eqs. 3.5 and 2.15. For  $\tan^2 \theta_i \leq 1/10$ , the ratio comes from Eq. 3.10, we can replace  $\tan \theta_i$  by its argument  $\theta_i$  with negligible error, and  $\Delta r_{gi}$  comes from combination of Eqs. 2.15 and 2.29,  $\Delta r_{gi} \doteq 2 \Delta z_i / (\sqrt{\theta_i^2 + 2D_i} + \theta_i)$ .

Putting these together gives

$$\Delta r_i = \begin{cases} \frac{1}{8} \frac{D_i^2}{\tan^3 \theta_i \sin^2 \theta_i} \Delta z_i & \text{if } \tan^2 \theta_i \geq 10D_i \\ \left( \frac{2}{\sqrt{\theta_i^2 + 2D_i} + \theta_i} - \frac{1}{\sqrt{\theta_i^2 + D_i}} \right) \Delta z_i & \text{if } \tan^2 \theta_i \leq 1/10. \end{cases}$$

4.5

(b) Calculation of  $\Delta t_i$ :

For  $\tan^2 \theta_i \geq 10D_i$ , the ratio is found from Eq. 3.6 and  $\Delta t_{vi} \doteq \Delta z_i / (c_i \sin \theta_i)$  results from Eq. 2.16. For  $\tan^2 \theta_i \leq 1/10$ , Eq. 3.11 yields the ratio and since angles are small  $\tan \theta_i$  can be replaced with  $\theta_i$ ; Eqs. 2.16 and 2.29 similarly yield  $\Delta t_{vi} \doteq \Delta z_i / (c_i \sqrt{\theta_i^2 + D_i})$ . Thus we have

$$c_f \Delta t_i = \begin{cases} \frac{1}{8} \frac{D_i^2}{\sin^3 \theta_i} \left( \frac{1}{\tan^2 \theta_i} + \frac{2}{3} - 2 \cos^2 \theta_i \right) \Delta z_i & \text{if } \tan^2 \theta_i \geq 10D_i \\ \left( \frac{2}{\sqrt{\theta_i^2 + 2D_i} + \theta_i} - \frac{1}{\sqrt{\theta_i^2 + D_i}} \right) \Delta z_i & \text{if } \tan^2 \theta_i \leq 1/10 \end{cases}$$

4.6

where simplification has been achieved by the additional approximation  $c_i \doteq c_f$  for all  $i$ . (For the values of  $c$  typically found in sea water, this approximation is good to within a couple per cent.)

(2) The Case  $d\theta = \Delta\theta/2$ .

We have seen that  $\Delta r_{vi} / \Delta r_{gi}$  is identically unity for all  $\theta_i$ ,

$$\Delta r_i = 0 \quad \text{all } \theta_i. \quad 4.7$$

Analysis for  $\Delta t_i$  proceeds as in the previous case except that Eqs. 3.16 and 3.18 are used instead of Eqs. 3.6 and 3.11. The results are

$$c_f \Delta t_i = \begin{cases} \frac{1}{12} \frac{D_i^2}{\sin^3 \theta_i} \Delta z_i & \text{if } \tan^2 \theta_i > 10D_i \\ \frac{1}{3} \theta_i \left( \frac{\sqrt{\theta_i^2 + 2D_i} - \theta_i}{\sqrt{\theta_i^2 + 2D_i} + \theta_i} \right)^2 \Delta z_i & \text{if } \tan^2 \theta_i \leq 1/10 \end{cases}$$

The formulas for these cases  $h = D/2$  and  $d\theta = \Delta\theta/2$  are summarized in Figure 4.2.

$\Delta Z = \sin \theta_f c_f \sum_{i=1}^f \Delta t_i$
$\Delta R = \sum_{i=1}^f \Delta \kappa_i - \cot \theta_f \Delta Z$

$$h = D/2$$

$$\Delta \kappa_i = \begin{cases} \frac{1}{8} \frac{D_i^2}{\tan^3 \theta_i \sin^2 \theta_i} \Delta z_i & \tan^2 \theta_i \geq 10D \\ \left( \frac{2}{\sqrt{\theta_i^2 + 2D_i} + \theta_i} - \frac{1}{\sqrt{\theta_i^2 + D_i}} \right) \Delta z_i & \tan^2 \theta_i \leq 1/10 \end{cases}$$

$$c_f \Delta t_i = \begin{cases} \frac{1}{8} \frac{D_i^2}{\sin^2 \theta_i} \left( \frac{1}{\tan^2 \theta_i} + \frac{2}{3} - 2 \cos^2 \theta_i \right) \Delta z_i & \tan^2 \theta_i \geq 10D \\ \Delta \kappa_i & \tan^2 \theta_i \leq 1/10 \end{cases}$$

$$d\theta = \Delta\theta/2$$

$$\Delta \kappa_i = 0$$

$$c_f \Delta t_i = \begin{cases} \frac{1}{12} \frac{D_i^2}{\sin^3 \theta_i} \Delta z_i & \tan^2 \theta_i \geq 10D \\ \frac{1}{3} \theta_i \left( \frac{\sqrt{\theta_i^2 + 2D_i} - \theta_i}{\sqrt{\theta_i^2 + 2D_i} + \theta_i} \right)^2 \Delta z_i & \tan^2 \theta_i \leq 1/10 \end{cases}$$

Figure 4.2

## B. Analysis for a Sample Profile

Assume that the receiving array is at a depth of 210 m, the source is at the surface, the speed of sound at the surface is  $1.5 \times 10^3$  m/sec,  $\Delta z$  is 3 m for every layer, and  $D = 2 \times 10^{-4}$  for all layers. This corresponds to a speed-of-sound profile which is nearly isogradient with  $g \doteq 0.1/\text{sec}$ .

The depth deficits  $\Delta Z$  and range deficits  $\Delta R$  of the source location were calculated for the two isospeed models as functions of the arrival angle  $\theta_r$  at the array. The calculations used the approximate equations in Figure 4.2. The results are presented in Table 4.3 and Figure 4.4.

For this sample profile, the condition  $\tan^2 \theta \geq 10 D$  is equivalent to  $\theta \geq 2.6^\circ$  and the condition  $\tan^2 \theta \leq 1/10$  is equivalent to  $\theta \leq 17^\circ$ . The pair of equations for  $\Delta r_i$  and the pair for  $\Delta t_i$  thus overlap for  $5^\circ \leq \theta \leq 10^\circ$ , since for this range of arrival angles all angles encountered along the ray paths lie between  $5^\circ$  and  $14^\circ$ . In this range of overlap, it is seen that the predicted values of  $\Delta Z$  and  $\Delta R$  from the different equations for each of the cases  $h = D/2$  and  $d\theta = \Delta\theta/2$  are in good agreement. The poorest agreement occurs for  $\Delta R$  in the case  $h = D/2$ . This results from the fact that for  $\tan^2 \theta_i \geq 10 D$  the expression for  $\Delta R$  is the difference of two large nearly equal quantities

$$\Delta R = \sum_{i=1}^f \Delta r_i - \cos \theta_f \sum_{i=1}^f c_f \Delta t_i$$

each of which is correct to within a few percent. The disagreement can be seen to be consistent with the approximations made in obtaining the large angle equation for  $\Delta r_i$ . As  $\theta_f$  increases the discrepancies in  $\Delta R$  decrease rapidly because the two terms become more dissimilar. This imprecision in  $\Delta R$  does not occur for the range  $\tan^2 \theta_i \leq 1/10$  because in this case



nominal values			$h = D/2$		$d\theta = \Delta\theta/2$	
$\theta_r$	$\theta_f$	$R_f$	$\Delta Z$	$\Delta R$	$\Delta Z$	$\Delta R$
0.0°	9.5°	2520 m	15 m	1.3 m	$3.3 \times 10^{-4}$ m	$-2.0 \times 10^{-3}$ m
0.1	9.5	2490	11	0.93	$5.3 \times 10^{-4}$	$-3.2 \times 10^{-3}$
0.2	9.5	2470	8.2	0.68	$6.0 \times 10^{-4}$	$-3.6 \times 10^{-3}$
0.5	9.5	2390	3.0	0.25	$5.7 \times 10^{-4}$	$-3.4 \times 10^{-3}$
1.0	9.6	2270	0.69	$5.7 \times 10^{-2}$	$3.7 \times 10^{-4}$	$-2.2 \times 10^{-3}$
2.0	9.7	2040	$9.8 \times 10^{-2}$	$8.3 \times 10^{-3}$	$1.9 \times 10^{-4}$	$-1.1 \times 10^{-3}$
5.0	10.8	1520	$6.4 \times 10^{-3}$	$5.9 \times 10^{-4}$	$5.7 \times 10^{-5}$	$-3.0 \times 10^{-4}$
			$6.5 \times 10^{-3}$	$9.9 \times 10^{-4}$	$5.9 \times 10^{-5}$	$-3.1 \times 10^{-4}$
10.0	13.8	1000	$7.0 \times 10^{-4}$	$8.5 \times 10^{-5}$	$1.9 \times 10^{-5}$	$-7.7 \times 10^{-5}$
			$6.7 \times 10^{-4}$	$1.8 \times 10^{-4}$	$2.0 \times 10^{-5}$	$-8.0 \times 10^{-5}$
20.0	22.1	550	$4.9 \times 10^{-5}$	$2.4 \times 10^{-5}$	$5.7 \times 10^{-6}$	$-1.4 \times 10^{-5}$
50.0	50.7	170	$9.6 \times 10^{-7}$	$2.2 \times 10^{-7}$	$1.2 \times 10^{-6}$	$-9.7 \times 10^{-7}$
70.0	70.3	80	$6.7 \times 10^{-7}$	$-1.8 \times 10^{-7}$	$7.9 \times 10^{-7}$	$-2.8 \times 10^{-7}$
90.0	90.0	0	$7.0 \times 10^{-7}$	0	$7.0 \times 10^{-7}$	0

$$D = 2 \times 10^{-4}$$

$$\Delta z = 3 \text{ m}$$

Array depth = 210 m

Source at the surface

$$c(\text{surface}) = 1.5 \times 10^3 \text{ m/sec}$$

Range and depth deficits for the two isospeed layer models.

Table 4.3

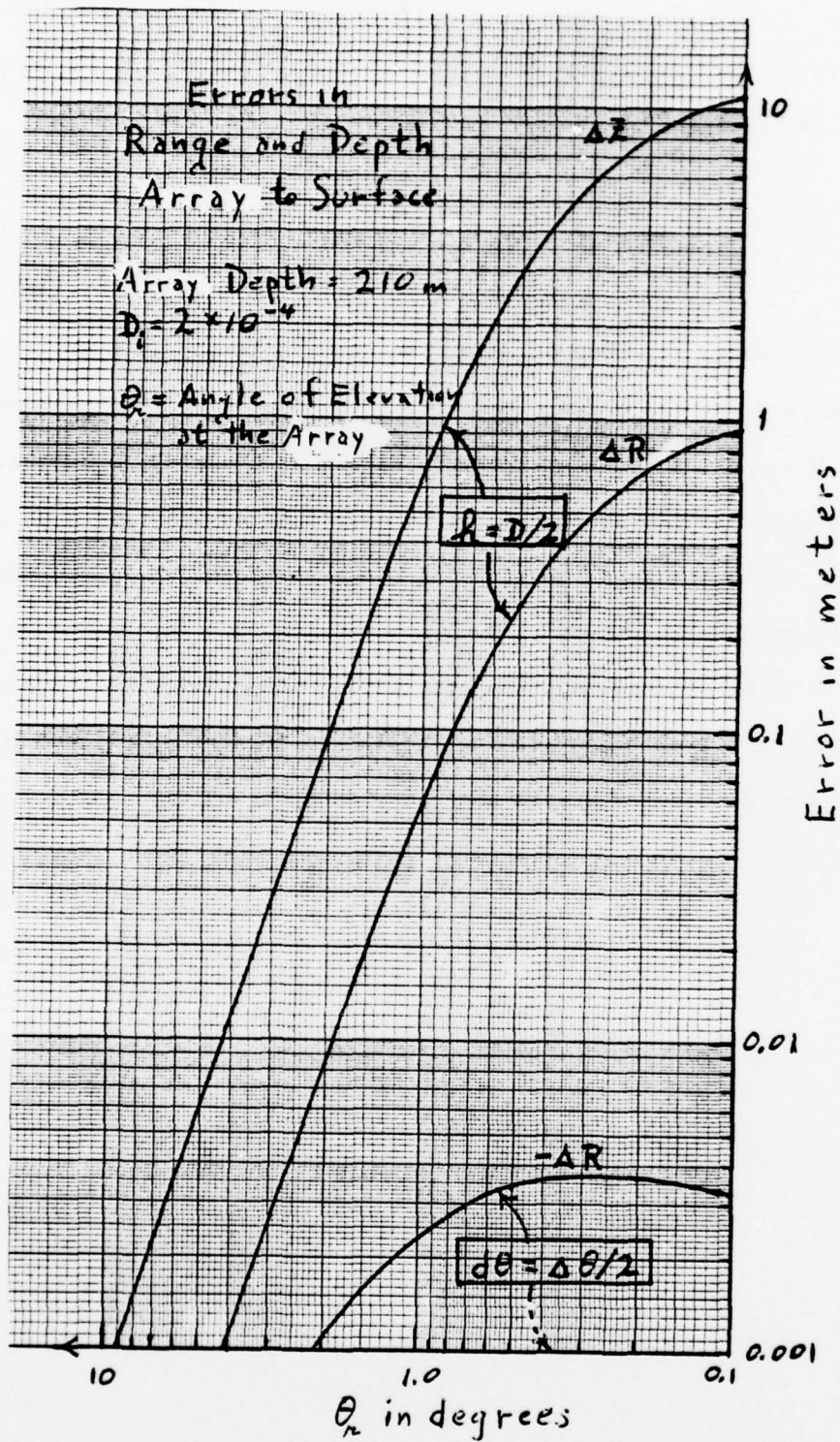


Figure 4.4

$c_f \Delta t_i = \Delta r_i$  so that

$$\Delta R = (1 - \cos \theta_f) \sum_{i=1}^f \Delta r_i$$

and the difference  $(1 - \cos \theta_f)$  does not involve  $\Delta r_i$  or  $\Delta t_i$ .

Figure 4.4 reveals quite clearly that the use of the isospeed model based on  $h = D/2$  results in very large errors at the extreme ranges. For the sample profile used here, it is seen that beyond ranges of 2000 m the error in the apparent range of the source approaches 1 m and the error in the apparent depth exceeds 1 m.

(It is to be noticed that the errors place the source too high and too near. This is a result only of the model used for traceback, and must be distinguished from other errors which may enhance, nullify, or reverse this tendency.)

## V. INITIALIZATION ERROR

A very important requirement for accurate localization of the source is the correct value for the ray invariant. An error in this quantity can arise from incorrect calculation of the angle of arrival  $\theta_r$  of the sound at the center of the array and from error in the choice of the value of the speed of sound  $c_r$  at the center of the array.

Since the ray invariant is  $\cos \theta_r / c_r$  it is clear that the effect of an incorrect  $\theta_r'$  is indistinguishable from that of an incorrect  $c_r'$ . Choosing the wrong value  $c_r'$  is equivalent to having the right  $c_r$  but the wrong  $\theta_r'$  if  $c_r'$  and  $\theta_r'$  are related by

$$\cos \theta_r' = \frac{c_r}{c_r'} \cos \theta_r \quad 5.1$$

If this wrong ray is traced back in isogradient water, the error  $\Delta r$  becomes

$$\Delta r = \Delta r_g - \Delta r_g'$$

where  $\Delta r_g'$  is for the incorrectly chosen ray. Use of (2.4) results in

$$\Delta r = \frac{c_r}{g \cos \theta_r} \left\{ (\sin \theta - \sin \theta_r) - \frac{\cos \theta_r}{\cos \theta_r'} (\sin \theta' - \sin \theta_r') \right\} \quad 5.2$$

Analogously, the timing error is

$$\Delta t = \Delta t_g - \Delta t_g'$$

which, with (2.5) yields

$$\Delta t = \frac{1}{g} \ln \left( \frac{1 + \sin \theta}{1 + \sin \theta_r} \frac{1 + \sin \theta_r'}{1 + \sin \theta_r'} \right) \quad 5.3$$



If we assume that the error in the speed of sound is very small, so that

$$\frac{c_r}{c'_r} = 1 + \epsilon \quad \epsilon \ll 1,$$

then manipulation of (5.1) reveals

$$\cos \theta'_r = (1 + \epsilon) \cos \theta_r$$

and, with the help of Snell's Law,

$$\frac{\cos \theta'}{c} = \frac{\cos \theta'_r}{c_r} = \frac{\cos \theta_r}{c_r} = \frac{c_r}{c'_r} \frac{\cos \theta_r}{c_r} = \frac{c_r}{c'_r} \frac{\cos \theta}{c} \doteq (1 + \epsilon) \cos \theta$$

or

$$\cos \theta' \doteq (1 + \epsilon) \cos \theta .$$

Substitution into (5.2) and (5.3) yields

$$\Delta t \doteq \frac{c_r}{g \cos \theta_r} \left\{ \frac{\epsilon}{\sin \theta} - \frac{\epsilon}{\sin \theta_r} \right\} \quad 5.4$$

and

$$\Delta t \doteq \frac{1}{g} \epsilon \left( \frac{1}{\tan^2 \theta} \frac{\sin \theta}{1 + \sin \theta} - \frac{1}{\tan^2 \theta_r} \frac{\sin \theta_r}{1 + \sin \theta_r} \right) \quad 5.5$$



The resultant range and depth deficits are then

$$\Delta Z = (\sin \theta) c \Delta t$$

$$\Delta R = \Delta h - \cot \theta \Delta Z$$

Since both  $\Delta t$  and  $\Delta h$  are proportional to  $\epsilon$ , we see that the errors in locating the source are linear in the fractional error  $\epsilon$  in the speed of sound  $c_r$  at the depth of the center of the array. These equations require  $\epsilon \ll \tan^2 \theta$ , but are reasonably accurate as long as  $\epsilon/(\tan^2 \theta) \leq 1/4$ .

As an example, let us assume that the array is at a depth of 210 m, at which  $c_r = 1521$  m/sec, and that the speed of sound at the surface is 1500 m/sec. This isogradient water has  $g = 0.1$ /sec and the situation is nearly equivalent to that analyzed in the preceding section. For a source at the surface, the range and depth deficits encountered for an error of 0.15 m/s in the speed of sound at the array ( $c'_r = 1520.85$  m/s) are presented in Figure 5.1.

Notice that for this underestimate of  $c_r$  the apparent location of the source is significantly too deep at extreme ranges. For the sample profile studied here, comparisons of these errors with those resulting from the isospeed model for which  $h = D/2$  reveals that an error in  $c_r$  of one part in  $10^4$  is far more serious than those resulting from either of the isospeed layer models for the speed of sound profile.

$\theta_r$	R nominal	$\Delta Z$	$\Delta R$
1°	2270	- 13 m	- 2.2 m
2	2040	- 5.8	- 1.0
5	1520	- 1.7	- 0.32
10	1000	- 0.56	- 0.14
20	550	- 0.15	- 0.060
50	170	- 0.014	- 0.018

$$c_r = 1521$$

$$c'_r = 1520.85$$

$$g = 0.1$$

Array depth = 210 m

Source at the surface

Approximate range and depth errors.

Table 5.1

## VI. RESULTS AND CONCLUSIONS

The analyses of the preceding sections reveal that:

(1) If an isogradient layer is modeled by an isospeed layer whose speed of sound  $c_v$  is the average over depth of the speed of sound  $c(z)$  in the isogradient layer,

$$c_v = \langle c_g \rangle = c \left( 1 - \frac{D}{2} \right) \quad 6.1$$

the trajectory line and time of flight through the layer can be seriously in error for rays whose angles of elevation are small.

(2) If in the isogradient layer the ray path has angle of elevation  $\theta$  upon entrance to, and  $\theta + \Delta\theta$  upon exit from, the layer, then if the straight line ray path in the isospeed layer has an angle of elevation of  $\theta + (1/2) \Delta\theta$ , the error in the trajectory (at entrance and exit) vanishes identically and the error in time of flight remains very small for all angles of elevation.

(3) A very small error in either  $\theta_r$  or  $c_r$  can introduce serious errors in localization of the source when the ray is nearly horizontal over some portion of its path.

Thus, the usual method of basing isospeed-layer models of isogradient layers on the average over depth of the speed of sound  $c_v = \langle c_g \rangle$  can lead to serious errors in the localization of the source of the sound if the ray becomes nearly horizontal anywhere on the path between source and receiver. If, on the other hand, the angle of elevation of the ray in each isospeed layer is required to be  $\theta + (1/2) \Delta\theta$ , where  $\theta$  and  $\theta + \Delta\theta$  are the entrance and exit angles of the ray in the isogradient layer, then the errors become acceptably small. It is worth noting that this approach can be shown to be equivalent to requiring  $c_v$  for the isospeed layer to be

given by

$$c_v = \langle c_g \rangle \left[ 1 + \frac{1}{8} \frac{(\Delta\theta)^2}{1 - \frac{D}{2}} \right] \approx c \left[ 1 - \frac{D}{2} + \frac{1}{8} (\Delta\theta)^2 \right] \quad 6.2$$

It is our opinion that better than either of these choices is to represent the "true" profile by isogradient layers for which the speed of sound is allowed to be discontinuous across the boundaries of the layers. This method of approximating the profile was suggested in Figure 1.1(b). It is to be noticed that this method should be more accurate than the more usually encountered constrained fit of Figure 1.1(c).

Finally, very small errors in the angle of elevation or speed of sound at the receiver can introduce large errors in localizing the source if the ray is nearly horizontal somewhere over its path. In particular, in positive-gradient water the most important part of the speed-of-sound profile is that closest to the bottom where the ray is most nearly horizontal.

INITIAL DISTRIBUTION LIST

	Copies
1. Defense Documentation Center Cameron Station Alexandria, Virginia 22314	2
2. Commanding Officer ATTN: Mr. R.L. Marimon (Code 70) Naval Torpedo Station Keyport, Washington 98345	6
3. Professor O.B. Wilson (Code 61W1) Naval Postgraduate School Monterey, California 93940	6
4. Dean of Research (Code 012) Naval Postgraduate School Monterey, California 93940	1
5. Library (Code 0434) Naval Postgraduate School Monterey, California 93940	2
6. Associate Professor Alan B. Coppens (Code 61Cz) Naval Postgraduate School Monterey, California 93940	4
7. Professor K.E. Woehler (Code 61Wh) Naval Postgraduate School Monterey, California 93940	1
8. Department Library (Code 61) Naval Postgraduate School Department of Physics & Chemistry Monterey, California 93940	1